PAPER • OPEN ACCESS

Solid by-products of a CF_3I–CO_2 insulating gas mixtures on electrodes after lightning impulse breakdown

To cite this article: P Widger and A Haddad 2017 *J. Phys. Commun.* **1** 025010

View the article online for updates and enhancements.

Related content

- Effects of reduced pressure and additives on streamers in white oil in long point-plane gap
  N V Dung, H K Høidalen, D Linhjell et al.

- Optimization of CFETR CSMC cabling based on numerical modeling and experiments
  Jinggang Qin, Chao Dai, Bo Liu et al.

- Development of dielectric barrier discharges
  Valentin I Gibalov and Gerhard J Pietsch

Journal of Physics Communications

PAPER

Solid by-products of a CF$_3$I–CO$_2$ insulating gas mixtures on electrodes after lightning impulse breakdown

P Widger[ID] and A Haddad

School of Engineering, Cardiff University, Queen's Building, The Parade, Cardiff, United Kingdom

E-mail: widgerp@cardiff.ac.uk

Abstract

This paper investigates the solid by-products of CF$_3$I–CO$_2$ gas mixtures and their proposed use as an alternative insulation medium in gas insulated switchgear and lines. The deposited by-products of a 30%–70% CF$_3$I–CO$_2$ gas mixture are experimentally investigated using stainless steel, aluminium and copper contacts whilst a standard 50 kV lightning impulse is used to cause electrical breakdown in the gas mixture. Following breakdown, the accumulated by-products over the electrodes surface were examined using an imaging microscope and scanning electron microscope. This paper discusses the results of microscope analysis on the surface of the electrodes and explores the effects that the detected by-products could have on high voltage CF$_3$I–CO$_2$ gas insulated equipment.

1. Introduction

Sulphur hexafluoride (SF$_6$) is the most reliable gas insulation medium used worldwide in the power industry in gas insulated switchgear (GIS) and gas insulated lines (GIL). SF$_6$ is used in the power industry because it has an insulation strength approximately three times that of air at atmospheric pressure which has led to compact and reliable GIS and GIL equipment [1]. SF$_6$ is also chemically inert and has advantageous arc extinction qualities. However, it is now widely known that the global warming potential (GWP) of SF$_6$ is extremely high, with a value of 23 900 times that of CO$_2$ [2]. SF$_6$ also has a reported atmospheric lifetime of 3200 years [2] which coupled with its infrared radiative capabilities has led to its extremely damaging effect on the environment when released into the atmosphere. It is important that any substitute insulating gas possess a high insulation strength at a relative low pressure whilst maintaining long term stability in any container. Furthermore, it is important that if any breakdown occurs in the gas, it can recover without a vast increase in by-products. If by-products occur that reduce or compromise the overall insulation capability of the gas, this could affect the long-term usefulness of any alternative insulation medium.

One alternative insulation gas that shows promising insulation properties to replace SF$_6$ is Trifluoroiodomethane (CF$_3$I) and its mixtures [3]. An important characteristic of CF$_3$I includes its ability to rapidly decompose in solar light which results in a GWP of less than 5 [4]. CF$_3$I also has an extremely short atmospheric lifetime of less than 2 days [4]. The result of CF$_3$I's short atmospheric lifetime and its very low GWP mean that its negative effect on the environment is virtually non-existent compared to SF$_6$.

Under uniform field conditions, it has been shown that CF$_3$I has a breakdown voltage 1.2 times that of SF$_6$ [4] and so could potentially be used to insulate future power equipment. It is, therefore, important that research, such as that conducted in this paper, examines the effects of breakdown on this new insulation medium and examines its deposited by-products when in close proximity to common materials used in GIS and GIL.

When examining the by-products of CF$_3$I, it is important to note that SF$_6$, which is currently used in the power industry, produces many by-products when subjected to a high voltage breakdown, such as SOF$_2$ (Thionyl Fluoride), SO$_2$ (Sulphur Dioxide), SO$_2$F$_2$ (Sulphuryl Fluoride), SOF$_4$ (Sulphur Oxide Tetrafluoride), SiF$_4$ (Silicon tetrafluoride) and CF$_4$ (Carbon Tetrafluoride) which can, in most cases, be removed using

Figure 1. Equivalent circuit diagram of experimental test setup.
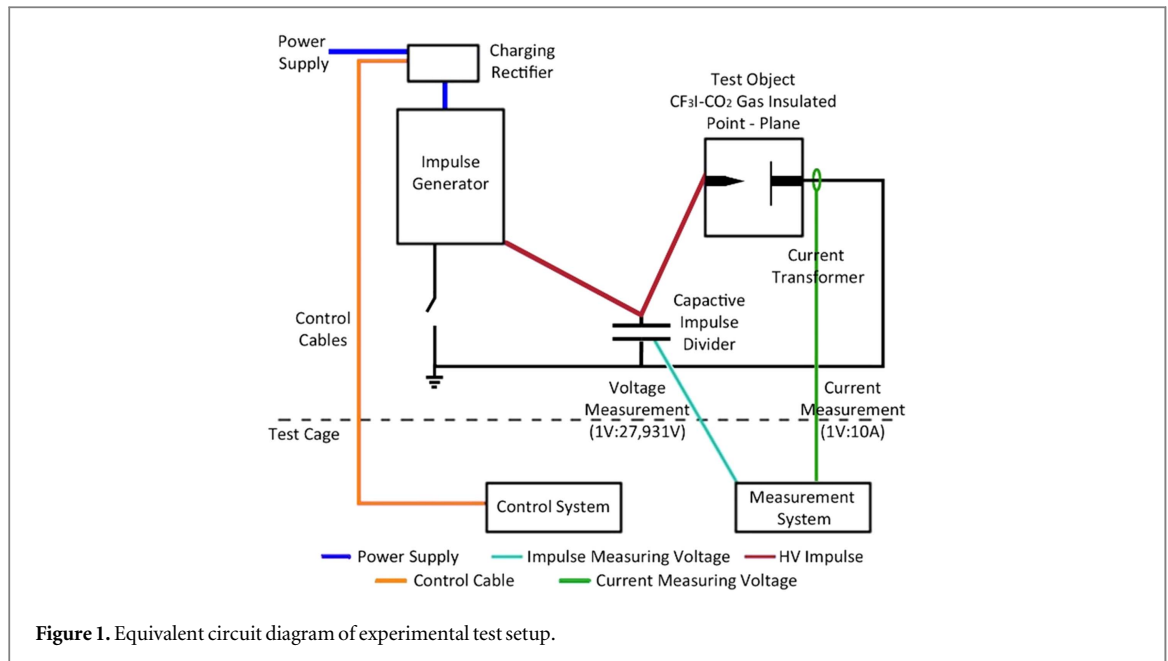
absorbents [5]. SF_6 also produces solid by-products during arcing such as metal fluoride (white) powders which are extremely acidic [5].

In this paper, the deposited surface by-products of a 30%–70% CF_3I–CO_2 gas mixture are examined following electrical breakdown due to lightning impulses being applied to a point-plane electrode configuration. These studies will help improve understanding of the process that takes place across gas gaps in switchgear [6] and GILs [7] if insulated by CF_3I–CO_2 gas mixtures. Research has shown that CF_3I–CO_2 gas mixtures are capable of insulating gas gaps in MV switchgear [6] and models of GILs [7]. However, little is known about the deposited by-products that gas breakdown could produce. In [8] the production of Iodine (I_2) is simulated and theorised from a CF_3I–CO_2 gas mixture but not experimentally proven by using an SEM/EDX as is shown in this paper. In [8, 9] the insulation characteristics of CF_3I–CO_2 gas mixtures is evaluated using partial discharge inception voltage. This paper examines the deposited surface by-products created during this process and further develops the process of detecting solid by products [10, 11]. This paper experimentally uses an SEM/EDX to identify the solid by-products produced by a CF_3I–CO_2 gas mixture, a task which has not previously been undertaken.
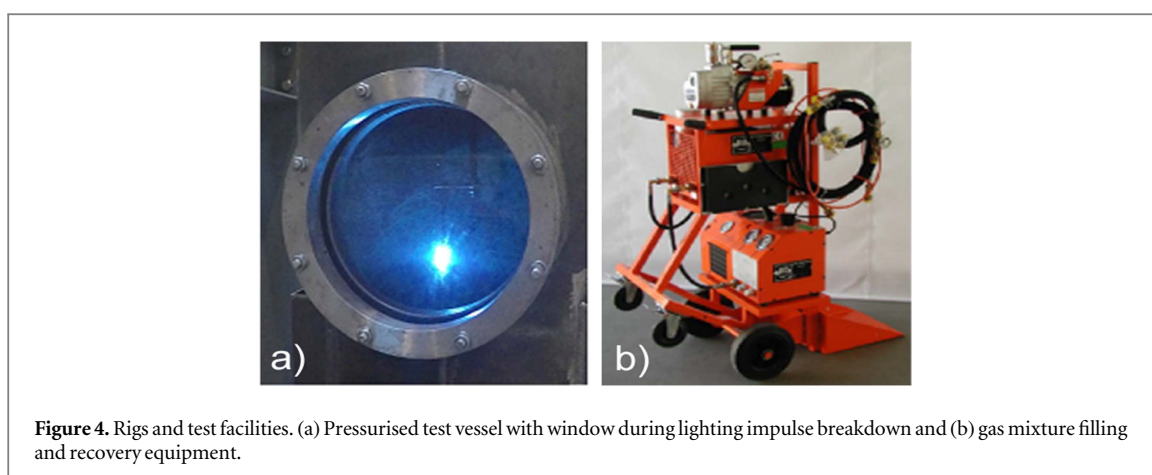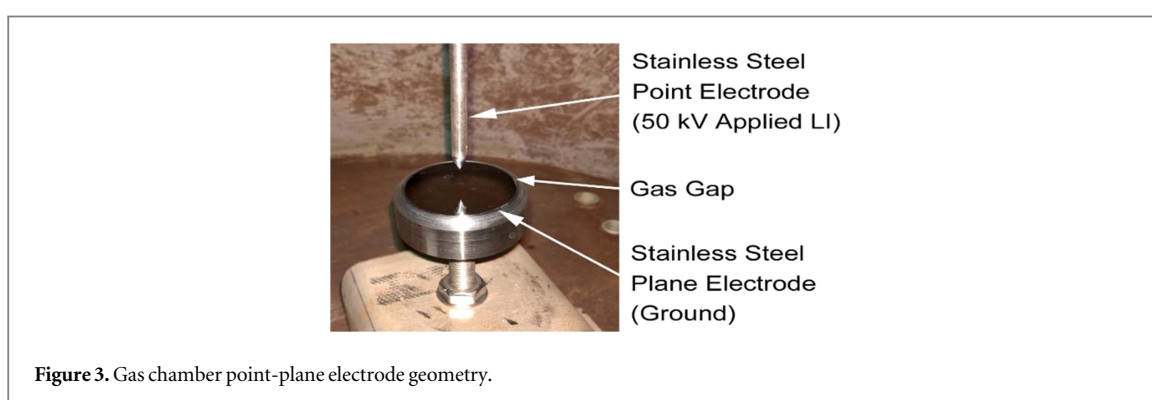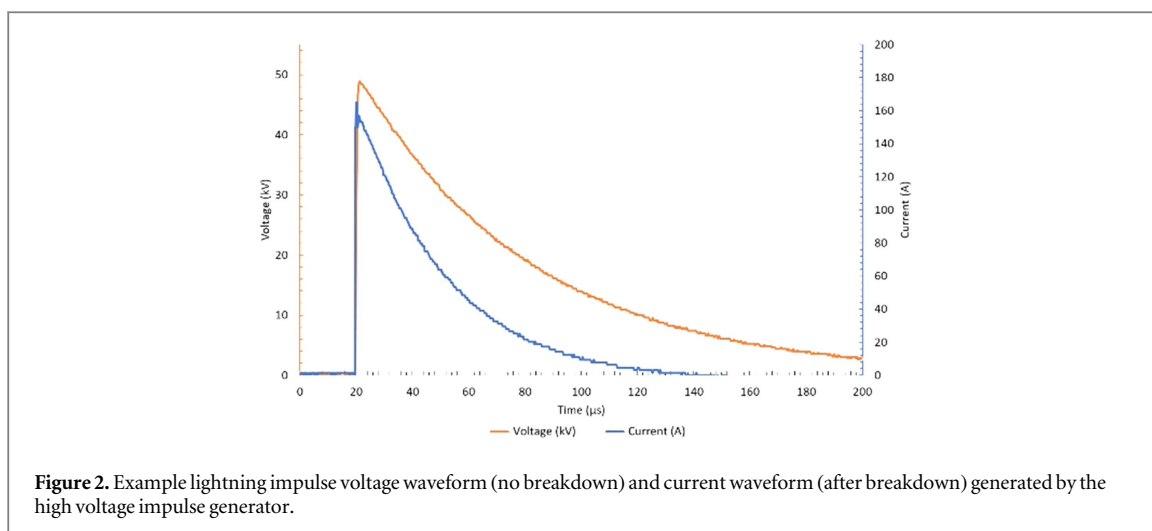
2. Experimental test setup

Throughout the experimental research conducted in the following sections, the deposited by-products produced on the surface of electrodes made of common GIS and GIL materials were investigated. In this experiment, a high voltage impulse generator was used to apply a 50 kV standard positive lightning impulse (1.2/50 μs), at a current level of 165 A, to the point electrode for all material types. The equivalent circuit diagram is shown in figure 1 and an example waveform of the voltage (no breakdown) and current (after breakdown) is shown in figure 2. The build-up of by-products was examined after breakdown events occurred. A gas mixture of 30%–70% CF_3I–CO_2 was used throughout the testing program with the gas insulation medium separating a point-plane electrode configuration as shown in figure 3.

In each experiment, the pressure vessel, shown in figure 4(a), contained the test electrode system and was evacuated using a vacuum pump. A gas mixture of 30%–70% CF_3I–CO_2 was then used to fill in the pressure vessel at a pressure of 0.15 MPa or 0.5 bar (above atmospheric pressure) and the breakdown test undertaken. After each breakdown test, the gas mixture was re-covered and re-used using the equipment shown in figure 4(b).

In order to test different materials, three point electrodes were constructed from 5 mm diameter stainless steel, aluminium and copper with a rod having a tip length of 10 mm. These point electrodes were each connected in turn to an air insulated bushing through which the lightning impulse was applied. In each system, the plane electrode was 45 mm in diameter with a rounded edge and is constructed from the same stainless steel, aluminium and copper alloys as the point electrode. An approximate inter electrode gas gap of 20 mm of 30%–70% CF_3I–CO_2 was then set between the electrodes for testing.

A Zeiss Axio Imager M2m imaging microscope was used to examine the surface defects of lightning impulses on each polished plane contact for each material. A Hitachi TM3030 scanning electron microscope (SEM/EDX)

Figure 2. Example lightning impulse voltage waveform (no breakdown) and current waveform (after breakdown) generated by the high voltage impulse generator.

Figure 3. Gas chamber point-plane electrode geometry.

Figure 4. Rigs and test facilities. (a) Pressurised test vessel with window during lighting impulse breakdown and (b) gas mixture filling and recovery equipment.

was also used to identify basic material elements of by-products that were deposited on the surface of the different electrodes after 1, 3 and 400 lightning impulse flashovers had been applied. The SEM/EDX analysis conducted after 1 lightning impulse shows the by-products produced from the gas mixture. Analysis after 3 impulses demonstrated that surface effects were repeatable. The use of 400 lightning impulse breakdowns allowed for the continued production of by-products to be demonstrated and analysis to show whether new by-products were produced in such quantities that they could not have been detected after only 1 breakdown.

3. Stainless steel electrode test results

This section utilises point-plane electrodes made from stainless steel. Stainless steel was chosen because previous research has indicated that when CF_3I is stored in close proximity to stainless steel, no degrading or chemical

Table 1. Chemical composition of stainless steel (grade 1.4307).

Element	% Present from specification [13]	% Present from SEM/EDX analysis
Chromium (Cr)	17.5–19.5	22.92
Nickel (Ni)	8.0–10.5	12.22
Manganese (Mn)	0.0–2.0	0
Silicon (Si)	0.0–1.0	0
Nitrogen (N)	0.0–0.11	0
Phosphorous (P)	0.0–0.05	0
Carbon (C)	0.0–0.03	0
Sulphur (S)	0.0–0.03	0
Iron (Fe)	Balance	64.85
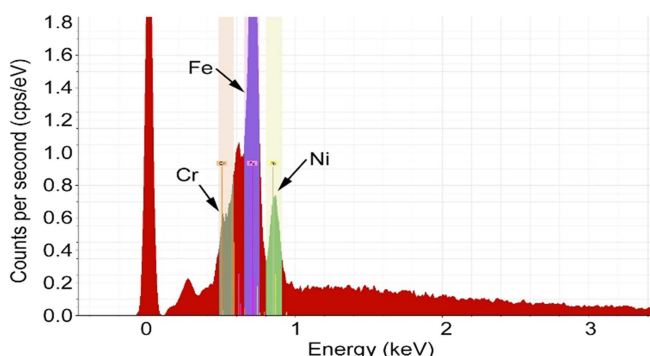
Figure 5. Stainless steel polished plane electrode SEM/EDX results—Iron (Fe)—64.85%, Chromium (Cr)—22.92%, Nickel (Ni)—12.22%.

interaction could be observed [12]. Stainless steel alloy grade 1.4301/304 (Commercial designation 304L) was chosen because of the relatively few elements that exist within its chemical composition in any large quantities as shown in table 1. Figure 5 shows the SEM/EDX examination result of a small area of the surface of the stainless steel electrode before any breakdown test was undertaken which also indicates the percentage of elements detected. As shown in table 1, the SEM/EDX results and the specified elements from the datasheet of the stainless steel alloy are in good agreement. The slight differences can be attributed to the limited viewing window of the SEM/EDX which is a small 2D surface. It is expected that slightly different compositions may be present for different surface areas of the same contact.

A single lightning impulse at 50 kV was then applied to the point electrode, and the voltage of the gas breakdown through the 30%–70% CF_3I–CO_2 gas mixture was measured using a capacitive impulse voltage divider. After the gas mixture had been recovered from the pressure vessel, the plane electrode was examined using the imaging microscope, and the resulting impact of the breakdown on the stainless steel plane contact is captured in figure 6. The same imaging microscope is further utilized under dark light conditions, as shown in figure 7, to highlight the exact surface defects that have been introduced as a consequence of the gas mixture breakdown onto the previously mirror finished electrode.

The same electrode is then analysed using the SEM/EDX and the center of the breakdown impact is shown in figure 8. The detected elements from the area displayed in figure 8 are shown in figure 9. By identifying the differences between figures 5 and 9, the new elements that are deposited on the stainless steel electrode surface due to a CF_3I–CO_2 gas mixture breakdown should be more identifiable. From the analysis undertaken using the SEM/EDX, it is clear that an increase in carbon deposits is identified and possible iodine deposition is seen. However, because the identifiable energy levels of iodine and chromium are very close to each other, it is quite difficult to distinguish between the two elements and identify exactly how much iodine might be deposited on the contacts surface as a result of breakdown in CF_3I gas mixtures.

Subsequent testing involved three lightning impulses impacting a new polished stainless steel plane electrode as shown in figure 10. This is important as the surface effects of each impulse can be seen to exhibit similar surface deformation/deposits and indicates the repeatability of the SEM/EDX results shown in figure 9. Each individual breakdown impact indicates a similar element percentage present in and around each area as that shown in figure 9. Figure 10 also shows how the surface of the stainless steel electrode, previously polished silver in colour, has been turned a brown colour around the breakdown arc impact area. Figure 11 shows the center of
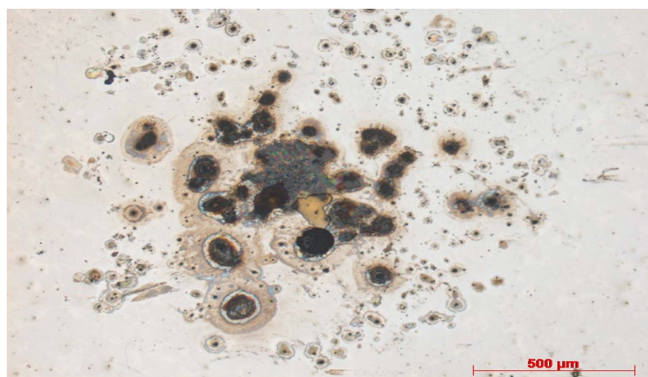
Figure 6. Polished stainless steel plane electrode after one lightning impulse breakdown to the surface as observed through an imaging microscope (bright light setting).
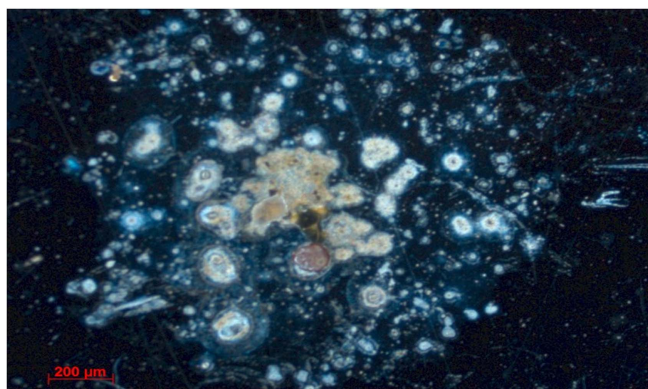

Figure 7. Polished stainless steel plane electrode after one lightning impulse breakdown to the surface as observed through an imaging microscope (dark light setting).
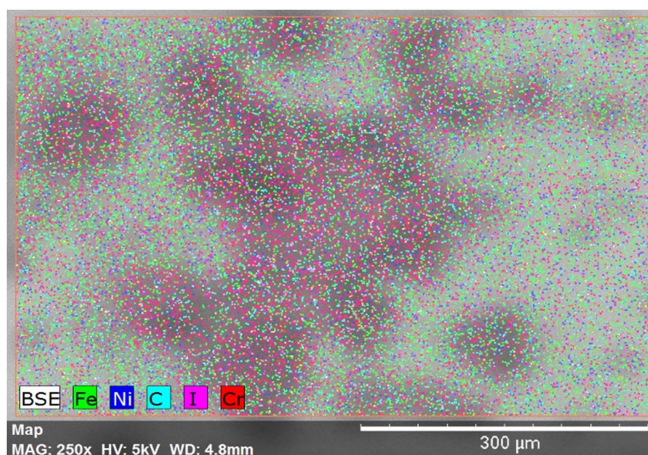

Figure 8. Stainless steel polished plane electrode after one lightning impulse breakdown to the surface as observed through the SEM/EDX—Carbon (C)—1.35%, Iodine (I)—61.89%, Chromium (Cr)—14.87%, Iron (Fe)—20.05% and Nickel (Ni)—1.81%.
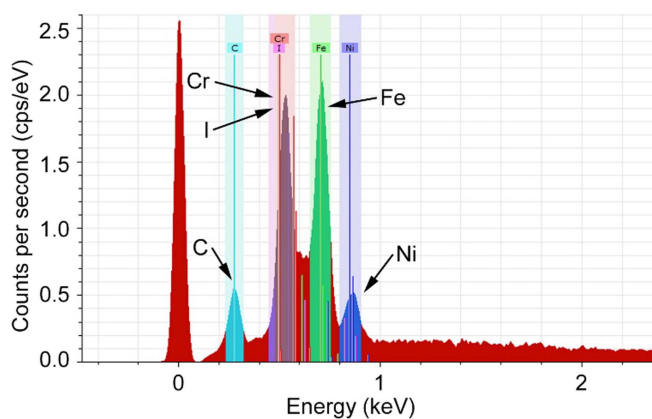
Figure 9. SEM/EDX results of the stainless steel polished plane electrode after one lightning impulse breakdown to the surface— Carbon (C)—1.35%, Iodine (I)—61.89%, Chromium (Cr)—14.87%, Iron (Fe)—20.05% and Nickel (Ni)—1.81%.
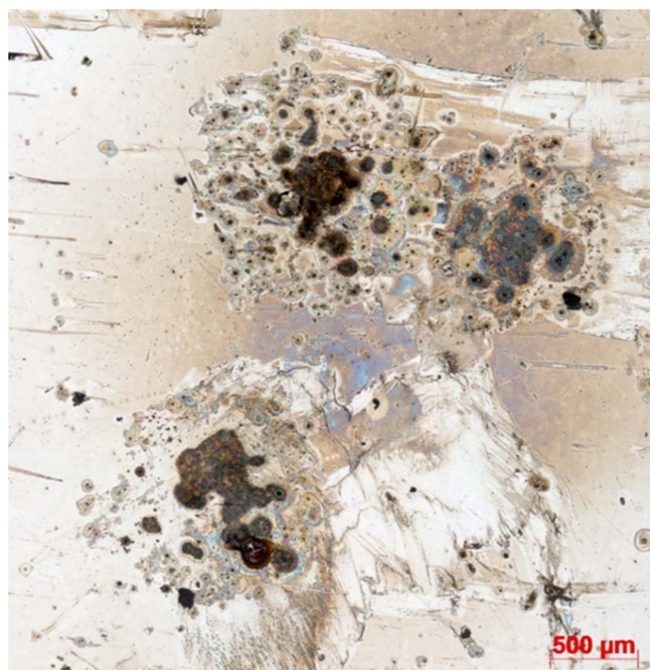

Figure 10. Polished stainless steel plane electrode after three successive lightning impulse breakdowns to the surface as observed through an imaging microscope (bright light setting).

one such impact which is also brown. This is important as deposits of iodine are often brown, as shown by the work carried out in [14].

4. Aluminium electrode test results

In this section, we report the surface examination results following CF_3I gas mixture breakdown in an aluminium point-plane electrode system. The results of surface degradation and deposits are examined when the aluminium electrodes are placed in a pressure vessel with a 30%–70% CF_3I–CO_2 gas mixture that undergoes breakdown when subjected to a 50 kV lightning impulse. The results with aluminium will be useful to evaluate the probable utilisation of CF_3I–CO_2 gas mixtures in gas insulated lines where aluminium is commonly used to manufacture the enclosure and central conductor [15]. The aluminium contacts in this research are manufactured from aluminium grade 6082/T6, and the specified percentage of alloy elements are shown in table 2.

Initially, the aluminium plane contact is examined under an imaging microscope after being polished to a mirror finish. It can be observed from figure 12 that the plane contact has more scratches than stainless steel.
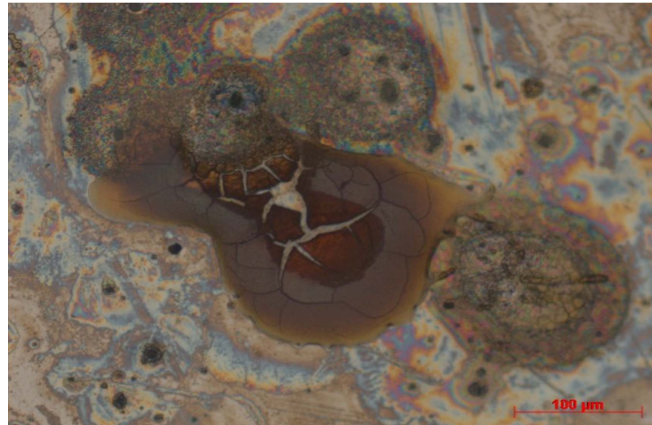
Figure 11. The center of a lightning impulse impact on a stainless steel polished plane electrode as observed through an imaging microscope (bright light setting). The area shown in figure 11. is shown as a dashed box in figure 10.

Table 2. Chemical composition of aluminium (grade 6082/T6).

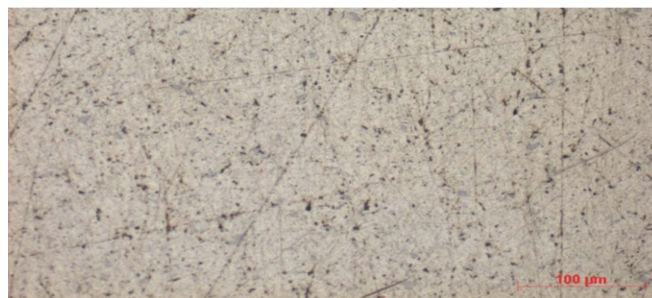| Element	% Present from specification [16]	% Present from SEM/EDX analysis
Silicon (Si)	0.70–1.30	1.73
Magnesium (Mg)	0.60–1.20	1.01
Mangenese (Mn)	0.40–1.00	7.62
Iron (Fe)	0.0–0.50	0
Chromium (Cr)	0.0–0.25	0
Zinc (Zn)	0.0–0.20	0
Others (total)	0.0–0.15	0
Aluminium (Al)	Balance	89.64

Figure 12. Polished aluminium plane electrode before a lightning impulse is applied as observed through an imaging microscope (bright light setting).

This is because aluminium is a softer alloy and is more susceptible to surface defects. After examination under the SEM/EDX, the results for detectable elements are shown in figure 13. These elements, as a percentage of a small area of the total surface, are shown in table 2. It can be shown that although most elements are present in similar values to those specified, the amount of manganese (Mn) present on the surface of the plane contact is higher than specified, and so may have an impact on the obtained results which are presented here.

Following the initial evaluation of the composition of the aluminium plane electrode, a single 50 kV lightning impulse was applied to the point aluminium electrode, which initiated breakdown across the 30%–70% CF_3I–CO_2 gas mixture. The resulting impact of the lightning impulse, on the aluminium plane contact, can be seen in figure 14. In general, it has been found that developing streamers branch out and propagate short distances to form corona in air [17], and it is likely that a similar process takes place in CF_3I–CO_2 gas mixtures. This branching process is clearly visible in figure 14. Figure 15 shows an enlarged image of the branching effect observed from the center of the breakdown across the surface of the aluminium under an imaging microscope.
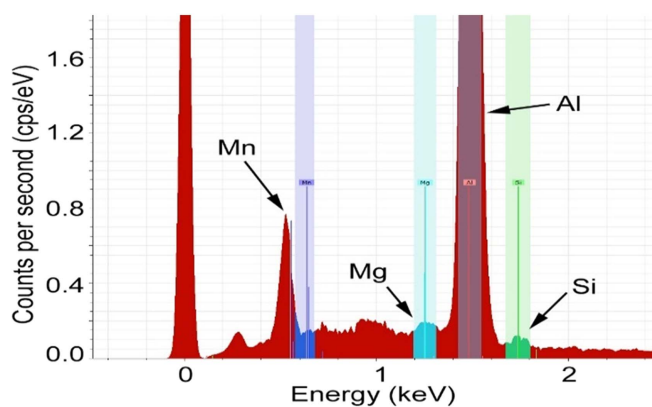
Figure 13. SEM/EDX results of an aluminium polished plane electrode before a lightning impulse is applied—Aluminium (Al)—89.64%, Manganese (Mn)—7.62%, Silicon (Si)—1.73%, Magnesium (Mg)—1.01%.
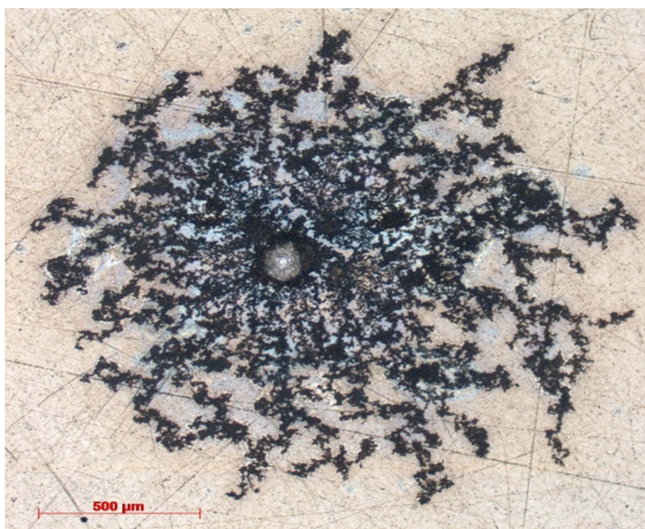

Figure 14. Polished aluminium plane electrode after 1 lightning impulse breakdown to the surface as observed through an imaging microscope (bright light setting).
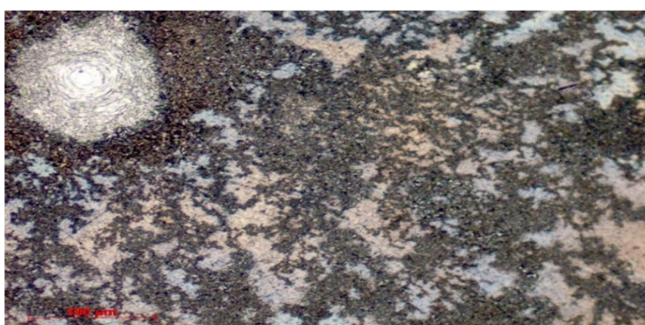

Figure 15. Polished aluminium plane electrode after 1 lightning impulse breakdown to the surface as observed through an imaging microscope showing branching effect (bright light setting).

Evaluation of this single lightning impulse breakdown on an aluminium contact under the SEM/EDX gives the image shown in figure 16. In this figure, it can be seen that there is a round central impact region. To the naked eye, this is brown in colour. The elements detected by the SEM/EDX are overlaid on the image and the distribution is shown in figure 17. As can be seen in figure 17, iodine is deposited across a large area of the
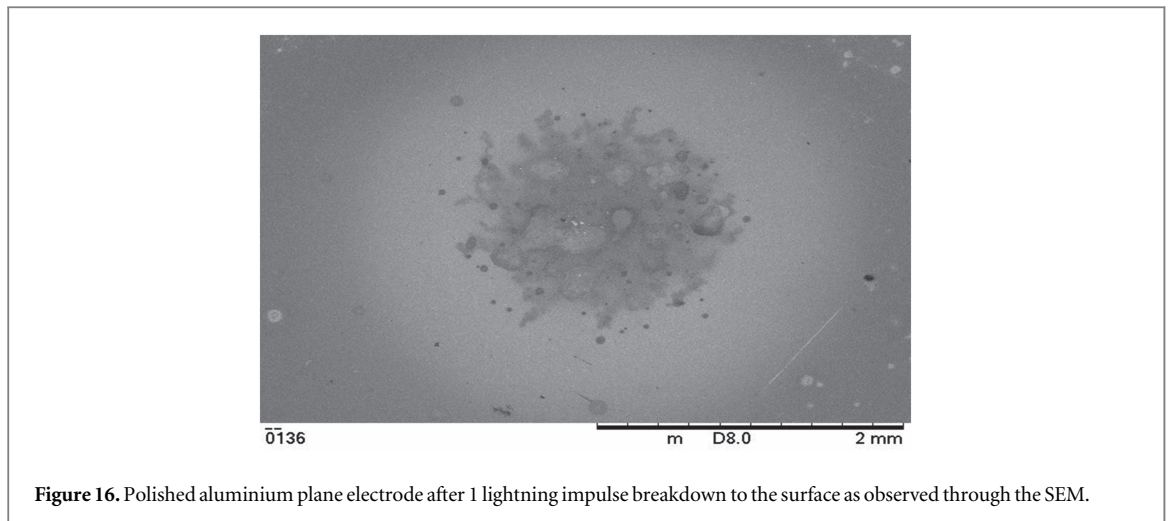
Figure 16. Polished aluminium plane electrode after 1 lightning impulse breakdown to the surface as observed through the SEM.
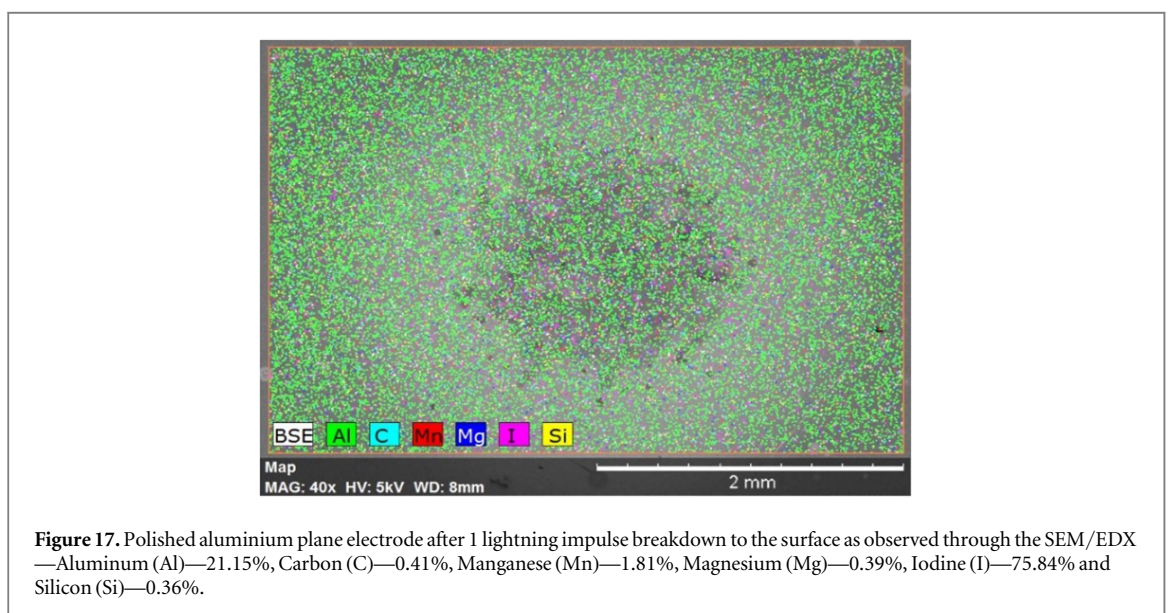

Figure 17. Polished aluminium plane electrode after 1 lightning impulse breakdown to the surface as observed through the SEM/EDX —Aluminum (Al)—21.15%, Carbon (C)—0.41%, Manganese (Mn)—1.81%, Magnesium (Mg)—0.39%, Iodine (I)—75.84% and Silicon (Si)—0.36%.
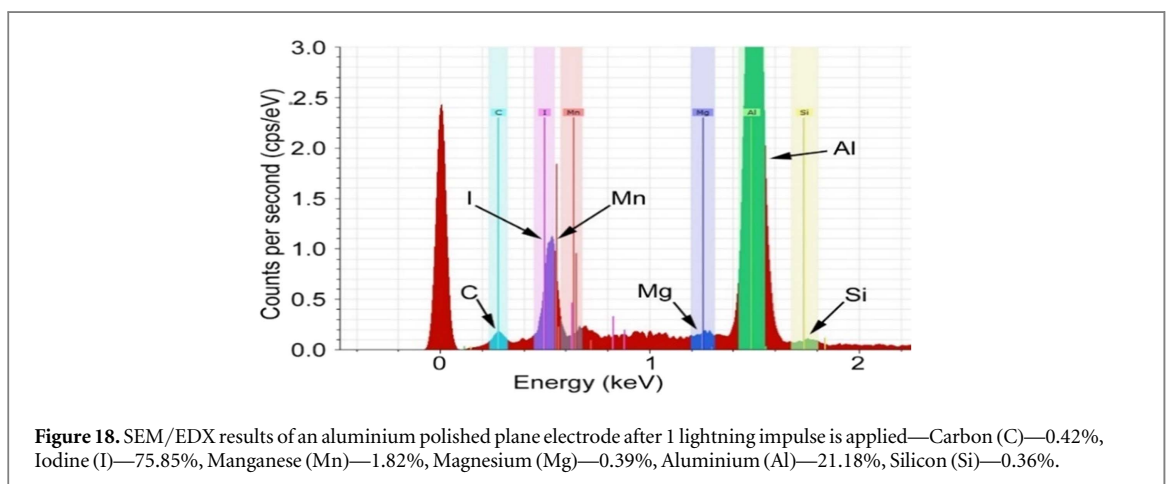

Figure 18. SEM/EDX results of an aluminium polished plane electrode after 1 lightning impulse is applied—Carbon (C)—0.42%, Iodine (I)—75.85%, Manganese (Mn)—1.82%, Magnesium (Mg)—0.39%, Aluminium (Al)—21.18%, Silicon (Si)—0.36%.

electrode, and it is not only concentrated at the centre of the breakdown impact region. This means that an absorbent for iodine may be needed to minimize or prevent detrimental effects inside GIS and GIL. Figure 18 shows the graphical representation of the elements shown in figure 17. It is important to note that a quick comparison of the percentage of elements found in figures 13 and 18 indicates that, although iodine is detected, the peak that represents the existence of manganese is in exactly the same energy region and it very difficult for

Table 3. Chemical composition of copper (CW004A).

Element	% Present from specification [19]	% Present from SEM/EDX analysis
Copper (Cu)	Balance	100
Other (total)	0.0–0.10	0

Figure 19. Polished copper plane electrode after 1 lightning impulse breakdown to the surface as observed through an imaging microscope (bright light setting).

the SEM/EDX to distinguish between the two elements. However, the percentage of elements shown on the surface of the contact in figure 18 seems to identify an increase in the amount of iodine detected on the surface of the electrode.

5. Copper electrode test results

In this section, copper electrodes were used for both the plane and point electrodes to examine the by-products deposited on these electrodes following the breakdown of a 30%–70% CF_3I–CO_2 gas mixture. Copper tungsten electrode tips are commonly used in GIS in order to prevent arcing deterioration [18], and so it is important to understand the by-products produced when copper electrodes and a CF_3I–CO_2 gas mixture are used.

The copper electrodes used in this investigation were all manufactured from copper commercial grade C1101/CW004A as shown in table 3. A sample of this copper was analysed using a scanning electron microscope (SEM/EDX), and the results of this are also shown in table 3. These results indicate that the electrode was made up almost entirely of copper and that, in the sample area, there may have been a small level of impurity, but the quantities of these elements were not large enough to register on the SEM/EDX analysis.

Initially, a single 50 kV lightning impulse was applied to the copper point electrode, which results in the point-plane electrode electric breakdown of the 30%–70% CF_3I–CO_2 gas mixture. The impact on the surface of the copper plane electrode can be seen in figure 19. Using the SEM/EDX, the elements extracted from figure 19 are shown in figure 20 where the elements detected are detailed and the presence of iodine is visible on the electrode surface. However, it is not present in sufficient quantities high enough to register clearly on the SEM/EDX.

Following this initial test, a new copper electrode was used. Three lightning impulses at 50 kV were applied to the plane electrode, and the surface effect of this is shown in figure 21.

In figure 22, an enlarged version of the central impact shown in figure 21 is displayed. A close-up of the branching effect of the impact on the surface of the copper electrode is shown in figure 23. When the surface breakdown impacts regions from figure 21 are compared against the image shown in figure 19, it can be shown that this impacted region is repeatable. SEM/EDX results of impacts shown in figure 21 also show that iodine is present across the surface of the plane electrode. However, the very small quantity makes it difficult to identify clearly.

After these initial lightning impulse tests through CF_3I–CO_2 gas, a copper electrode with 400 lightning impulse breakdowns at 50 kV was tested and analysed. Four hundred lightning impulses were applied with the objective to produce larger quantities of by-products which should be easier to identify positively. The copper
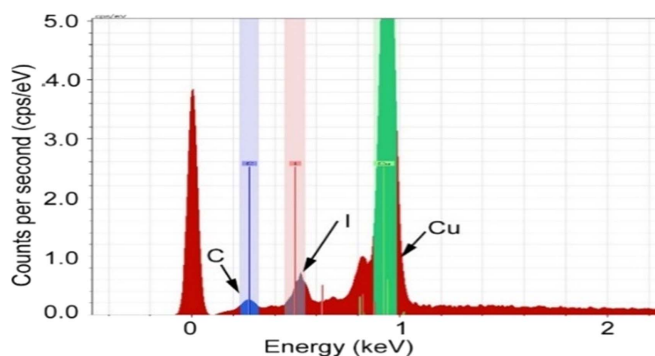
Figure 20. SEM/EDX results of a copper polished plane electrode after 1 lightning impulse is applied—Iodine (I)—51.81%, Copper (Cu)—47.37%, Carbon (C)—0.81%.
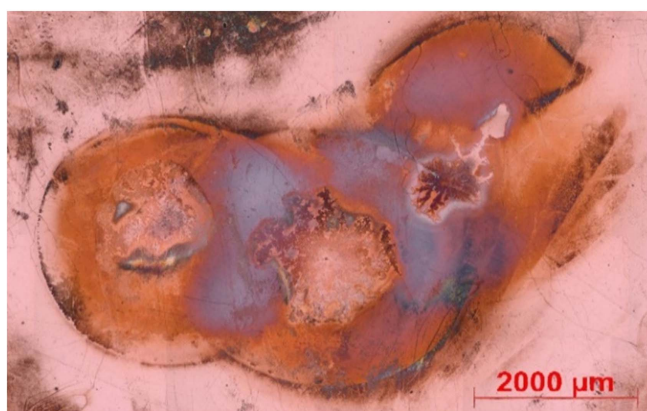

Figure 21. Polished copper plane electrode after 3 successive lightning impulse breakdowns to the surface as observed through an imaging microscope (bright light setting).
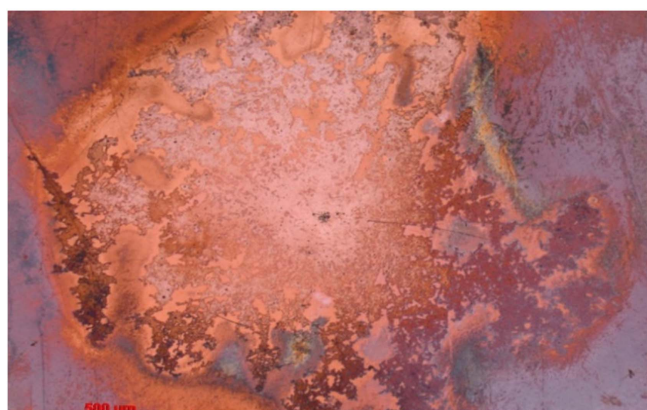

Figure 22. Polished copper plane electrode after 3 successive lightning impulse breakdowns to the surface as observed through an imaging microscope showing one of the impacted regions (bright light setting).

electrode surface with four hundred lightning impulse impacts from breakdown through the 30%–70% CF_3I–CO_2 gas mixture is shown in figure 24, where it is clear that all lightning impulses attached at the centre of the electrode and none impacted close to the edge of the electrode. The central region of breakdown impacts is shown in figure 25. It is important to note that the branching effect shown in figure 23 is no longer visible in figure 25 because of the extent of breakdown impacts in this small region.

The central region shown in figure 25 is examined using the SEM, as shown in figure 26. This image is then analysed for constituent elements, as shown in figure 27. From figure 28, it is evident that iodine is now present
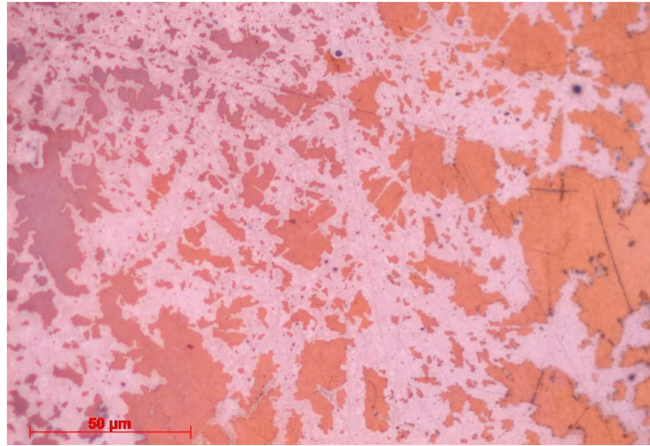
Figure 23. Polished copper plane electrode after three lightning impulse breakdown to the surface as observed through an imaging microscope showing branching effect (bright light setting).
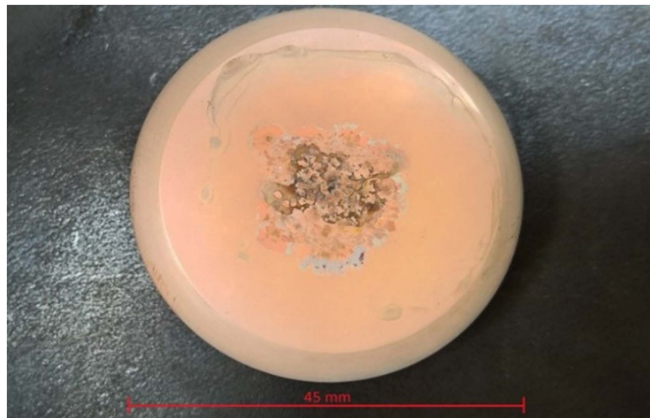

Figure 24. Polished copper plane electrode after 400 successive lightning impulse breakdowns to the surface.
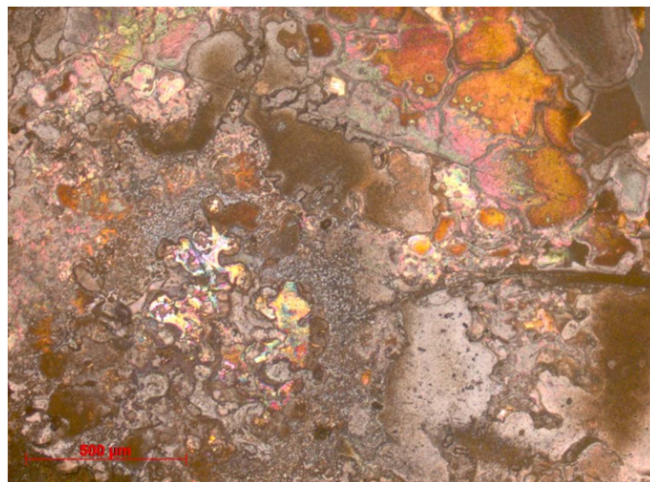

Figure 25. Polished copper plane electrode after 400 successive lightning impulse breakdowns to the surface as observed through an imaging microscope showing the central impact region (bright light setting).
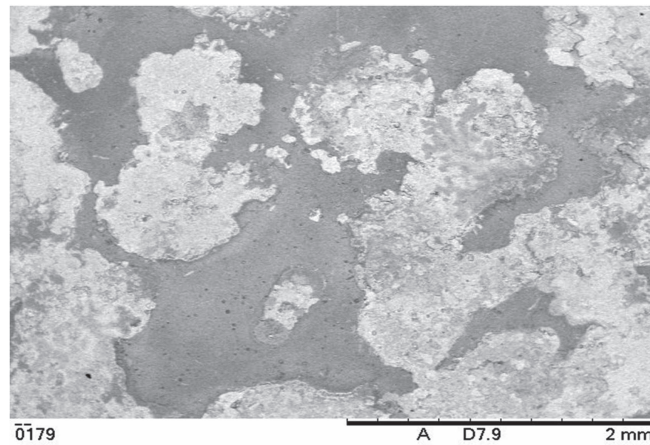
Figure 26. Polished copper plane electrode at the center after 400 lightning impulse breakdowns to the surface as observed through the SEM.
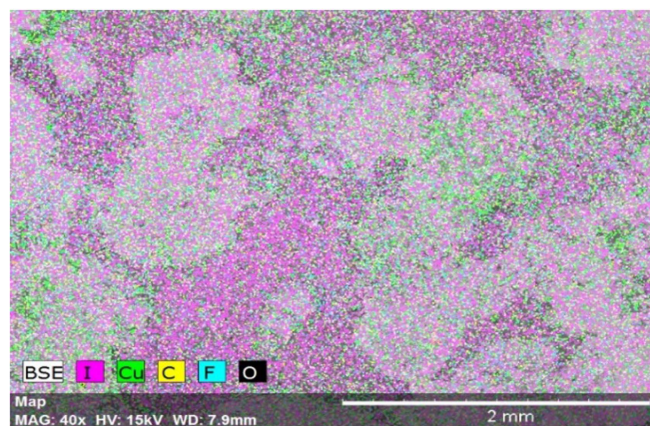

Figure 27. Polished copper plane electrode at the center after 400 lightning impulse breakdowns to the surface as observed through the SEM/EDX—Iodine (I)—48.54%, Copper (Cu)—42.26%, Oxygen (O)—6.68%, Carbon (C)—1.39%, Fluorine (F)—1.13%.
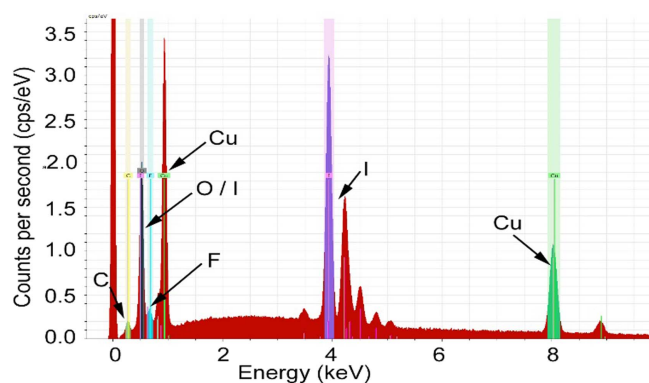
Figure 28. SEM/EDX results of a copper polished plane electrode at the center after 400 lightning impulses have been applied—Iodine (I)—48.54%, Copper (Cu)—42.26%, Oxygen (O)—6.68%, Carbon (C)—1.39%, Fluorine (F)—1.13%.

at the centre of the electrode. Iodine is positively identified by the initial peak at energy level 0.5 keV in figure 28 and also by the subsequent peaks around 4 keV which clearly indicate the iodine's unique presence.

SEM/EDX analysis was also undertaken on the edge of the copper electrode that was subjected to 400 gas breakdowns. The elements present on the surface clearly indicate that iodine is spread not only around the center of the electrode but also at the edges. After examining the iodine deposited on the electrode, it is clear that

Table 4. Summary of added elements on electrode surface.

Electrode material	1 and 3 breakdowns	400 breakdowns
Stainless Steel	Chromium affects Iodine detection	—
Aluminium	Manganese affects Iodine detection	—
Copper	Iodine (low quantity)	Iodine

a light covering can be observed on the electrode but not in large quantities. It is likely that iodine separates from CF_3I in the hot temperature inside the leader arc inbetween the point-plane electrode geometry when this is more than 457.4 K or 184 °C, which is the boiling point of iodine [20]. Once the iodine separates from CF_3I, it boils into a gas form and then spreads throughout the pressure vessel, when the iodine gas sufficiently cools below 386.85 K or 114 °C [20], it will change phase to solid and deposit on any surface, including the electrodes within the vessel. If this iodine could be absorbed during its gaseous state, it could be completely removed from GIS and GIL equipment and subsequently pose little problems for CF_3I–CO_2 gas mixtures use in power equipment.

6. Discussion

This paper examines the interaction of 30%–70% CF_3I–CO_2 gas mixtures with aluminium, stainless steel and copper electrodes when a 50 kV lightning impulse breakdown occurs across an electrode gap. The results are summarised in table 4. The results show that, with stainless steel contacts, brown deposits are left on the surface and that iodine is detected using an SEM/EDX. However, the chromium within the contacts makes it difficult to detect the exact by-products and in what percentage they are produced. When aluminium electrodes are used, a breakdown through the gas mixture clearly produces a branching pattern from the point of impact across the surface of the plane electrode. When surface deposits are analysed using the SEM/EDX on the aluminium contact, iodine was detected as a by-product. However, due to the manganese in the contact, it is difficult to define clearly the exact by-product element.

Copper electrodes were also examined and, because of the purity of the electrode, it was easier to identify deposits of iodine on the surface of the electrode. However, it took four hundred impulses to produce iodine in a quantity that was recognisable. Four hundred impulses is approximately equivalent to half the operations of a rated gas insulated switch disconnector on the network today, which is rated for 1000 operations [21]. This means that throughout a piece of switchgear's lifetime, insulated by a 30%–70% CF_3I–CO_2 gas mixture, it would be unlikely that iodine would be produced in large quantities. However, because of the low current of these impulses, it is possible that iodine may be produced in larger quantities in real-life equipment if high current arcs are present.

With the copper electrodes, the SEM/EDX indicates that the iodine is deposited in a widespread area which would make the use of an absorbent easier in GIS and GIL equipment, especially during iodine gaseous state when heated.

7. Conclusion

This paper experimentally demonstrates the effect of 50 kV lightning impulse breakdowns across a 30%–70% CF_3I–CO_2 gas mixture in order to evaluate the solid by-products produced. It is shown that iodine is produced in small quantities as a solid by-product after 400 breakdowns. However, it is difficult to detect as a by-product after 1 or 3 breakdowns.

When using stainless steel or aluminium electrodes, it is difficult to detect iodine using an SEM/EDX as alloy components affect clear detection. However, iodine is easier to detect on copper electrodes. It was observed and shown experimentally that iodine was spread in a wide area inside the pressure vessel tested. This indicates that iodine is produced as a gas inside the hot breakdown arc before cooling to become a solid deposited by-product. This paper demonstrated the likely effect of a breakdown within GIS/GIL equipment which is insulated with a CF_3I–CO_2 gas mixture and the resulting iodine by-products from a breakdown event. If an absorbent could be used to absorb iodine during its gaseous state, it would likely have little impact on the lifetime insulation of a piece of GIS or GIL. Future work will examine the gaseous by-products that are produced by CF_3I–CO_2 gas mixtures through the use of gas chromatography and mass spectrometry.

Acknowledgments

ORCID iDs

P Widger ⬤ https://orcid.org/0000-0002-0662-8590

References

[1] Farish O, Judd M D, Hampton B F and Pearson J S 2004 SF$_6$ insulation systems and their monitoring *Advances in High Voltage Engineering* (*IEE Power and Energy Series* 40) ed A Haddad and D Warne vol 40 (London: The Institute of Electric Engineers) pp 37–76

[2] Intergovernmental Panel on Climate Change (IPCC) 2008 Working Group I Contribution to Fourth Assessment Report of The IPCC —Intergovernmental Panel on Climate Change *Addendum-Errata of Climate Change 2007—The Physical Science Basis IPCC* WG1 AR4 Report Intergovernmental Panel on Climate Change (IPCC): Geneva, Switzerland

[3] Kumarudin M S, Chen L, Widger P, Elnaddab K H, Albano M, Griffiths H and Haddad A 2014 CF$_3$I gas and its mixtures: potential for electrical insulation *Conf.: Cigre Session 45 (Paris)*

[4] Taki M, Maekawa D, Odaka H, Mizoguchi H and Yanabu S 2007 Interruption capability of CF$_3$I gas as a substitution candidate for SF$_6$ gas *IEEE Trans. Dielectr. Electr. Insul.* **14** 341–6

[5] Koch D 2003 SF$_6$ properties, and use in MV and HV switchgear Schneider Electric. http://schneider-electric.com (Accessed: 01 May 2013)

[6] Widger P, Haddad A and Griffiths H 2016 Breakdown performance of vacuum circuit breakers using alternative CF$_3$I-CO$_2$ insulation gas mixture *IEEE Trans. Dielectr. Electr. Insul.* **23** 14–21

[7] Chen L, Widger P, Kamarudin M S, Griffiths H and Haddad A 2015 Potential of CF$_3$I gas mixture as an insulation medium in gas-insulated equipment *2015 IEEE Conf. on Electrical Insulation and Dielectric Phenomena (CEIDP) (Ann Arbor, MI)* pp 868–71

[8] Zhang X, Xiao S, Han Y and Dai Q 2015 Analysis of the feasibility of CF$_3$I/CO$_2$ used in C-GIS by partial discharge inception voltages in positive half-cycle and breakdown voltages *IEEE Trans. Dielectr. Electr. Insul.* **22** 3234–43

[9] Zhang X, Xiao S, Zhou J and Tang J 2014 Experimental analysis of the feasibility of CF$_3$I/CO$_2$ substituting SF$_6$ as insulation medium using needle-plate electrodes *IEEE Trans. Dielectr. Electr. Insul.* **21** 1895–900

[10] Widger P, Chen L and Haddad A 2016 Deposited by-products of CF$_3$I-CO$_2$ gas mixtures after lightning impulse flashover *Universities' Power Engineering Conf. (UPEC) (Portugal)*

[11] Xiao S, Li Y, Zhang X, Tang J, Tian S and Deng Z 2017 Formation mechanism of CF$_3$I discharge components and effect of oxygen on decomposition *J. Phys. D: Appl. Phys.* **50** 155601–13

[12] Donelly M K, Harris R H J and Yang J C 2004 *CF$_3$I Stability Under Storage National Technical Information Service (NIST) Technical Note* 1452 Technology Administration, US Department of Commerce, Springfield

[13] Aalco 2016 Stainless Steel 1.4307 Bar and section Specifications Aalco Metals Ltd. http://aalco.co.uk/datasheets/ (Accessed: 16 May 2016)

[14] Takeda T, Matsuoka S, Kumada A and Hidaka K 2007 By-products of CF$_3$I produced by spark discharge *Presented at Japan-Korea Joint Symp. on Electrical Discharge and High Voltage Engineering* (Shibaura Institute of Technology, The University of Tokyo) paper 17A-p7, pp 157–60

[15] Siemens A G and Energy Sector 2012 Gas-Insulated transmission lines (GIL) High-power transmission technology. http://w3.usa. siemens.com/smartgrid/us/en/events/Documents/IEEE%202016/TS_Gas-Insulated%20Transmission%20Lines.pdf (Accessed: 11 August 2017)

[16] Aalco 2016 Aluminium Alloy 6082—T6 Extrusions Specifications Aalco Metals Ltd. http://aalco.co.uk/datasheets/ (Accessed: 16 May 2016)

[17] Allen N L 2004 Mechanisms of air breakdown *Advances in High Voltage Engineering* (*IEE Power and Energy Series* 40) ed A Haddad and D Warne vol 40 (London: The Institution of Electric Engineers) pp 1–35

[18] Stewart S 2004 *Distribution Switchgear* (*IEE Power and Energy Series* 46) ed A T Johns and D F Warne (London, UK: The Institution of Electrical Engineers (IEE))

[19] Aalco 2016 Copper CW004A Sheet, Plate and Bar Aalco Metals Ltd. http://aalco.co.uk/datasheets/ (Accessed: 16 May 2016)

[20] Royal Society of Chemistry 2016 Periodic table—Iodine Royal Society of Chemistry. http://rsc.org/periodic-table/element/53/ iodine (Accessed: 04 July 2016)

[21] Schneider Electric 2011 Technical Characteristics Catalogue: Fluokit Air insulated switchgear up to 24 kV. Schneider Electric. http:// schneider-electric.com/products/ww/en/3500-mv-switchgear/3520-air-insulated-switchgear-for-secondary-distribution/60704- fluokit-m-24kv/?xtmc=fluokit%2520m24%252B&xtcr=1 (Accessed: 20 September 2013)